Available online at www.sciencedirect.com

SCIENCE DIRECT®

Journal of Marine Systems 54 (2005) 245–260

JOURNAL OF MARINE SYSTEMS

www.elsevier.com/locate/jmarsys

Paleoclimatic evolution of the Galician continental shelf (NW of Spain) during the last 3000 years: from a storm regime to present conditions

R. González-Álvarez[a,*], P. Bernárdez[a], L.D. Pena[a], G. Francés[a], R. Prego[b], P. Diz[a], F. Vilas[a]

[a]*Departamento de Geociencias Marinas y O.T., Facultad de Ciencias del Mar, Universidad de Vigo, 36200 Vigo, Pontevedra, Spain*
[b]*Grupo de Biogeoquímica Marina, Instituto de Investigaciones Marinas (CSIC), 36208 Vigo, Spain*

Received 20 March 2002; accepted 1 July 2004
Available online 25 September 2004

Abstract

A multiproxy study of the sedimentary record carried out on gravity core CGPL00-1 retrieved from the outer Galician continental shelf (NW of Spain) has allowed us to establish the main climate fluctuations affecting the region during the Upper Holocene. Grain size, TOC, C/N ratio, biogenic opal and planktonic foraminifera are the main analysed parameters. Lithology and grain size distribution lead to identify two sedimentary sequences: a lower half mainly composed by glauconitic sand and a muddy upper half. A chronology has been established based on three AMS radiocarbon ages, 907 cal. BC, 898 cal. BC and 1399 AD, and the aforementioned sedimentary sequences. The obtained radiocarbon ages are the first dated sediment samples for the Galician continental shelf. Geochemical markers show different trends in both sequences: low and/or fluctuating values in the sandy sequence and high and relatively constant values in the upper muddy sequence. The whole sandy interval is interpreted to be a nearly instantaneous deposit from a distal storm ebb current. The muddy interval was deposited in a stable and low-energy marine environment, similar to that found on the present outer shelf. The shift from a storm-dominated shelf to a low-energy environment took place synchronous with the Subboreal/Subatlantic transition, when an increase in storminess appears related to climatic instability. Transitional planktonic foraminiferal assemblage dominates the whole record, although a change to more abundant cold water species at 1420 AD, may relate to an intense upwelling pulse, probably reinforced by colder atmospheric temperatures during the Little Ice Age (LIA). Despite the presence of an upwelling regime since 1420 AD, lesser amount of opal has accumulated in the outer shelf due to enhanced offshore transport and stronger remineralization.

Keywords: Paleoclimatology; Holocene; Subboreal/Subatlantic transition; Planktonic foraminifera; Storminess; Upwelling; Galician continental shelf

* Corresponding author. Tel.: +34 986 812633; fax: +34 986 812556.
E-mail address: raquelg@uvigo.es (R. González-Álvarez).

0924-7963/$ - see front matter © 2004 Elsevier B.V. All rights reserved.
doi:10.1016/j.jmarsys.2004.07.015

1. Introduction

Understanding factors affecting climate change in the Holocene is of considerable importance: the topic being the subject of much current research and debate in relation to future climate change. Several climatic oscillations have characterized the last 3000 years. The most important has been identified at the Subboreal/Subatlantic transition, at around 850 cal. BC (van Geel et al., 1996), characterized by a shift from a relatively warm climate to cool and wet conditions in mid-latitudes (Kilian et al., 1995; van Geel et al., 1999). The first warm period in the last 3000 years coincides with the Roman Warm Period peaking at 100 AD (Bianchi and McCave, 1999) with a return to cold conditions after the fifth century in the Dark Ages (Lamb, 1995). In the last millennium, the best identified climatic fluctuations are the Medieval Warm Period (MWP), 900–1250 AD (Lamb, 1995), and the Little Ice Age (LIA), 1350–1800 AD (Stuiver et al., 1995).

These climatic oscillations have been registered by several authors in a large variety of records, for example in Greenland ice cores (Meese et al., 1994; O'Brien et al., 1995; Kreutz et al., 1997; Dahl-Jensen et al., 1998), North Atlantic deep sea cores (Keigwin, 1996; Bond et al., 1997; Bianchi and McCave, 1999), subtropical deep sea cores (deMenocal et al., 2000), lake sediments (Campbell et al., 1998), peat bogs (Barber et al., 2000) and tree rings (Edwards et al., 2000). However, paleoclimate records from shallow marine areas are very scarce. Records from such areas provide decisive information connecting continental with deep sea records. High sedimentation rates in these areas allow for detailed reconstructions in terms of temporal resolution, but the establishment of an accurate chronology in these environments is difficult thus hindering correct interpretation of the sedimentary record.

The present study is based on material from a 96 cm gravity core (CGPL00-1) retrieved from the outer Galician continental shelf (NW of Spain,

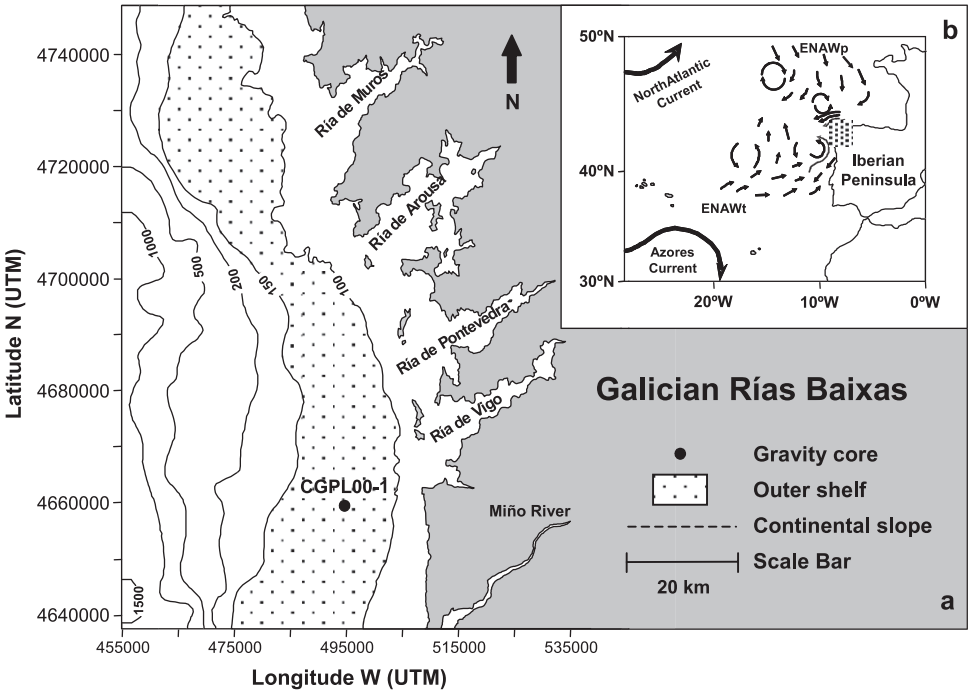

Fig. 1. Location of the study area (Galician Rías Baixas, NW Iberian Peninsula): (a) Western Galician continental shelf and location of core CGPL00-1. Depth contours in meters. (b) Schematic coarse view of ENAW distribution, including the regions of formation of $ENAW_p$ and $ENAW_t$, in the North Atlantic Ocean (simplified from Ríos et al., 1992).

42°5′15.115″N, 9°3′46.380″W, 130.8 m water depth, Fig. 1a). Grain size, organic carbon, organic carbon/total nitrogen ratio, biogenic opal and planktonic foraminifera are the main parameters constituting this multiproxy study. The aim of the present work is to integrate these geochemical and micropaleontological proxies in order to reconstruct environmental factors (water dynamics, storminess, water column productivity, etc.) and their evolution during the last 3000 years in the western Galician outer continental shelf.

2. Regional setting

The study area (Fig. 1a) extends between 41°53′ and 42°53′ latitude N and 8°35′ and 9°32′ longitude W, and represents a climatic province in mid-latitude region, strongly influenced by the position of the polar front. The oceanography of the western Galician coast is affected by wind-driven upwelling that is common along the eastern boundary of the North Atlantic between 10°N and 44°N (Wooster et al., 1976). The seasonal evolution of the Iberian upwelling is closely related to the large-scale climatology of the Northeastern Atlantic. During summer, when the Azores high-pressure cell is located in the central Atlantic and the Greenland low has diminished in intensity, the resulting pressure gradient forces air southward along the Iberian coast and induces upwelling. In contrast, in winter, the Azores high-pressure cell is located off the northwestern African coast and a deep low is located off the southeastern coast of Greenland. The pressure gradient between the two pressure systems results in an onshore wind and the appearance of a surface poleward flow (Haynes et al., 1993; Frouin et al., 1990).

Fraga (1981) described the presence of a quasi-permanent upwelling off the Galician coast from April to August that may persist until October. Nutrient input from this seasonal upwelling (Prego et al., 1999) is the main factor governing high productivity in this area (Fraga, 1981; Blanton et al., 1984; Prego and Bao, 1997). The upwelled seawater is the Eastern North Atlantic Central Water (ENACW) defined by Fiúza (1984), which has two different origins, named by Ríos et al. (1992) as Subpolar Eastern North Atlantic Water ($ENAW_p$) and Subtropical Eastern North Atlantic Water ($ENAW_t$). Both water masses could affect the Galician shelf according to the scheme shown in Fig. 1b where the limit of influence between them has been identified to the north of Cape Finisterre (Prego and Varela, 1998). The natural eutrofication of the western Galician waters by upwelling events is recorded in the shelf surface sediments by high values of opal content and *Chaetoceros* resting spores (Prego and Bao, 1997; Bao et al., 1997).

Sedimentary cover in the study region consists of thin (ranging from 2 to 6 m thick) sandy and muddy Quaternary sediments (Rey, 1993) in a wedge-shaped layer thinning to the outer shelf. There are no previous data concerning the sedimentary characteristics and internal chronology of this unit.

3. Materials and methods

The gravity core used in this work was recovered on board the B/O Mytilus during a cruise in May 2000. The core was sealed just after collection and kept in storage at 4 °C until analyses were performed in the laboratory. The core was split longitudinally in two sections and 1 cm thick slices were removed for radiographical analyses with a Cabinet X-ray System (Faxitron Series, Hewlett-Packard). After splitting, the core was visually described and sampled. One section was used for sedimentological analyses and the other employed for micropaleontological analyses and determination of opal content.

Correlative subsamples of 2 cm thickness were taken for grain size analyses. After removing the organic matter with H_2O_2, the coarse fraction was wet sieved and separated from the fine fraction with a 63-μm mesh sieve. The >63-μm residue was dry sieved through 2-, 1-, 0.5-, 0.250-, 0.125- and 0.063-mm sieves and weighed. Mud content was determined following the method outlined by McManus (1991). X-ray nephelometry (Micromeritics, Sedigraph 5100) was used to separate silt and clay.

Evaluation of total carbon (TC), total nitrogen (TN) and total inorganic carbon (TIC) content were performed with a Leco CC-100 CN 2000. Total organic carbon (TOC) was estimated by subtracting the inorganic carbon to the total carbon. Calcium carbonate content ($CaCO_3$) was calculated by multi-

plying the TIC by a constant factor of 8.33. Additionally, the TOC/TN ratio (hereafter C/N ratio) was calculated.

The remaining half of the core was sampled every centimetre for high resolution counts of planktonic foraminifera and measurements of opal content.

Opal in the sediments was extracted following the rapid wet alkaline solution procedure outlined by Mortlock and Fröelich (1989). Silica was extracted into 2M Na_2CO_3 solution at 85 °C for 5 h. The resulting extract was measured for the dissolved silicate concentration according to Hansen and Grashoff (1983). Finally, the percentage of opal in dry sediment is obtained following the expression:

$$\%\text{opal} = \frac{(C_m - C_0) \times 100}{P} \times K$$

where C_m is the dissolved silicate concentration of the sample in μM, C_0 is the dissolved concentration of the blank in μM, P is the dry sediment weight in μg and K (2.7 l g mol^{-1}) is a constant value comprising the digestion volume (l), the molecular mass of Si (g mol^{-1}) and a correction factor that depends on the opal water content. Measurements of opal content were carried out on bulk sediment and <63-μm fraction. The analytical deviation of the method was determined analysing two or more replicates of each sample, striving for a deviation below ±0.2%.

Samples for micropaleontological analyses were oven dried at 60 °C, weighed, disaggregated with 10 ml of sodium hexametaphosphate solution and washed over 63- and 125-μm mesh sieves. Samples were again dried and weighed. Counts on planktonic foraminifera fauna were conducted on samples collected every 5 cm, although samples were taken every 1 cm at several critical intervals to improve the resolution. The >125-μm fraction was split until an appropriate quantity of foraminifera was obtained for counting. More than 300 specimens from each sample were handpicked and identified under a stereoscopic binocular microscope following Kennett and Srinivasan (1983). With these data, relative and absolute abundances were calculated. Relative abundance is expressed as the percentage of each species in relation to the total specimens counted. The absolute abundance is the number of planktonic foraminifera per gram of dry sediment. The total number of benthic foraminifera in each sample was also counted to determine the planktonic/benthic foraminiferal ratio (PF/BF).

4. Results

4.1. Core description

Gravity core CGPL00-1 presents two well-differentiated sections (Fig. 2a). An intense bioturbation was observed throughout the core, especially in some critical intervals around 80 and 70 cm. The lower half consists mainly of sand overlaying a basal 2 cm interval of bioclastic gravel. Internal laminations were observed in this sandy interval, although sometimes obscured by bioturbation. The lamination is clearly visible on X-ray radiographies from 91 to 79 cm. Glauconite mean percentage in the sandy interval reaches 9%. Interlayered within this trend there are zones with a relatively higher percentage of mud, described as sandy mud. A drastic change in sediment composition was observed at 55 cm. This shift is characterised by a short interval of muddy sand followed by green mud deposits to the top of the core. Glauconite content at this muddy interval decreases upward falling to 3% as a mean value.

4.2. Grain size distribution

Grain size along the whole core presents a general decreasing trend from the bottom to the top. Gravel fraction is relatively abundant (9%) at the core bottom and negligible along the rest of the core (Fig. 2b). The most abundant sand fractions are fine and very fine sand (Fig. 2c,d), whereas coarse and medium sand are relatively scarce (<3%). The total sand abundance decreases progressively from 85%, at the core bottom, to 20% at the middle part of the core. From this level to the top of the core the sand content is almost constant, although a subtle increase can be seen in the uppermost 15 cm. The finest fractions show an inverse distribution illustrating, in general terms, a progressive enrichment from bottom to top. This trend is clearly exhibited by the medium and fine silt fractions (Fig. 2f). The percentage of very coarse and coarse silt fractions is irregular (Fig. 2e), punctuated by fluctuations ranging from 5% to 38%, although an upwards increasing trend may be inferred. The clay

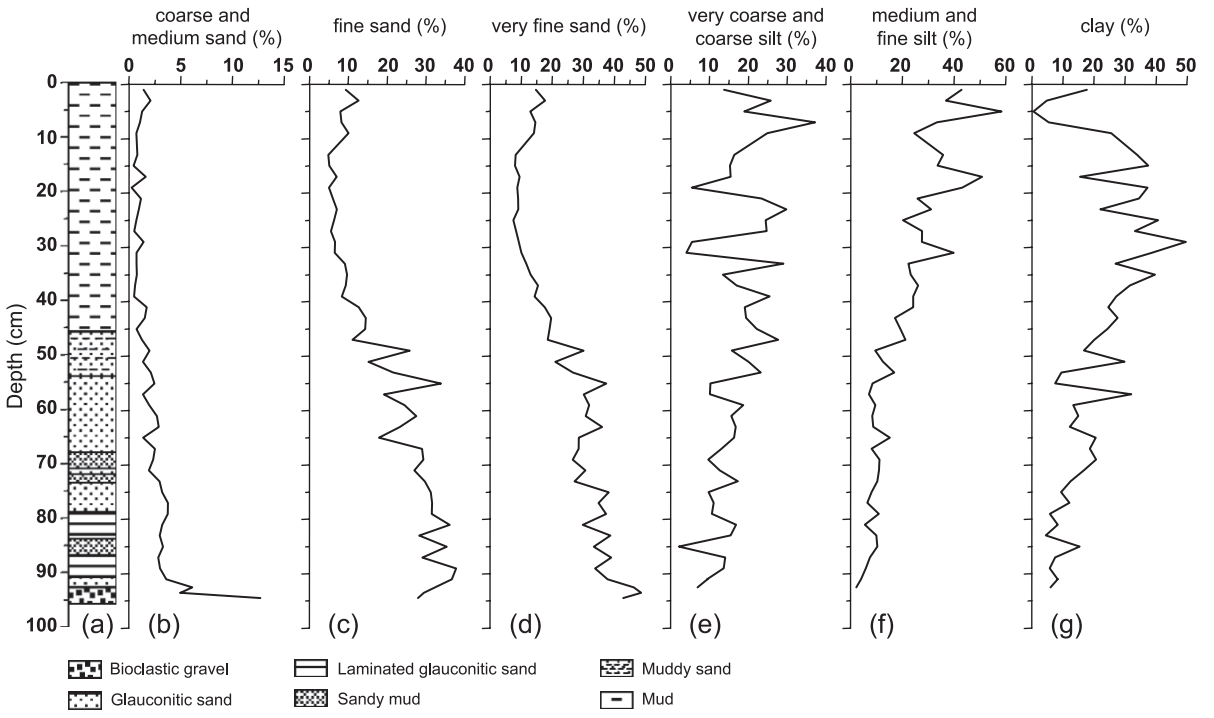

Fig. 2. Sedimentological features of core CGPL00-1: (a) Lithology and sedimentary structures. (b) Percentage of coarse and medium sand. (c) Percentage of fine sand. (d) Percentage of very fine sand. (e) Percentage of very coarse and coarse silt. (f) Percentage of medium and fine silt. (g) Percentage of clay.

fraction distribution (Fig. 2g) is clearly opposite to those of very coarse and coarse silt, registering the highest values (25–50%) from 40 to 10 cm.

To summarise, the complete section represents a fining upwards sequence embracing two smaller sequences: the decreasing grain size from bioclastic gravel to silty clay sediments (96–30 cm) constitutes a finning upwards sequence overlaid by a coarsening upwards sequence marked by the decrease of clay abundance, an increase of medium and fine silt, and a weak increment of sand fractions (30–0 cm).

4.3. Age model

The chronological framework of core CGPL00-1 is based on four accelerator mass spectrometry (AMS)-^{14}C ages. AMS analyses were performed at Geochron Laboratories (Cambridge, MA, USA). Dated levels are located at 26–28, 60–61, 70–71 and 95–96 cm. The latter is situated at the core bottom and the ^{14}C analysis was performed on a shell of *Acanthocardia* cf. *aculeata* (Linné, 1758). The remaining three samples were performed on planktonic foraminiferal tests. A monospecific sample of *Globigerina bulloides* was taken at 70–71 cm. Due to the impossibility of recovering only one species to carry out the analysis from the other two levels, a mixed *Neogloboquadrina pachyderma* (right-coiling) and *G. bulloides* sample was handpicked at 60–61 cm. The same problem arises at 26–28 cm, recovering a collection of mixed foraminifera.

Raw radiocarbon ages were calibrated using the Calib 4.3 program (Stuiver et al., 1998a,b). The global marine reservoir correction was applied. The resulting calibrated BP ages were converted into calendar years AD/BC (Table 1).

Soares (1993) suggests a change in hydrographic dynamics along the Portuguese coast between 1300 and 1100 BP that caused a significant increase in coastal upwelling off Portugal, reaching present intensities after 1100 BP. Due to this, Soares proposed that for these or younger ages, a local reservoir effect correction must be taken into account due to ^{14}C content impoverishment in upwelled waters. The

Table 1
Radiocarbon dates and calibrated ages from core CGPL00-1 (Geochron Laboratories)

Depth (cm)	Lab. number	Sample type	Measured radiocarbon age	Calibrated age BP	Age range (1σ)	Calendar age (AD/BC)
26–28	GX-28823-AMS	Mixed planktonic foraminiferal tests	1260±40	551	621–521	1399 AD
60–61	GX-28824-AMS	*N. pachyderma* (right-coiling) and *G. bulloides*	3090±40	2847	2894–2788	898 BC
70–71	GX-28627-AMS	*G. bulloides*	3100±40	2856	2915–2807	907 BC
95–96	GX-26928	Bivalve shell (*A.* cf. *aculeata*)	10,150±270	10,982	11,372–10,593	9033 BC

The age estimations were derived from the intercepts of the radiocarbon age plus and minus one time the total standard deviation of the age with the linear interpolation of the marine calibration data set. A local reservoir effect of 280±35 radiocarbon years was applied for the uppermost dated sample.

estimated local reservoir effect on the northern Portuguese coast is ΔR=280±35 years (Reimer, 2001). An upwelling intensification around 1000 AD in the Galician Rías Baixas, close to the core location, has also been described by Diz et al. (2002). Therefore, we applied the aforementioned reservoir effect to sample from 26 to 28 cm since the radiocarbon age falls within the age range given by Soares (1993), and represents the closest value to core location (250 km).

There are two alternative interpretations for the large difference between the 10,982 years BP bivalve shell age at 95–96 cm and the 2856 years BP foraminiferal shells age obtained at 70–71 cm: (1) The bivalve shell from the core bottom is in situ. Well-preserved delicate morphological elements and absence of surface abrasion signals support this option. If this statement is correct, a stratigraphic discontinuity should be inferred at the top of the bioclastic gravel interval. However, visual observations of the sediment and X-ray radiographies do not confirm the existence of this sedimentary discontinuity. (2) The shell is reworked and the age does not correspond to the age of the sediment in which it is found. The presence in this core of only one valve and the fact that this species has been reported in the region from relatively shallow muddy sand bottoms (Rolán-Mosquera et al., 1989) leads us to consider this second possibility as the most realistic. In this scenario, the bioclastic gravel interval and the overlying glauconitic sand would have been deposited in continuity. The age model has been elaborated considering this hypothesis and the described sedimentary sequences, applying linear sedimentation rates between foraminiferal dated samples and the limits of sequences.

The age model for core CGPL00-1 is depicted in Fig. 3. Ages for 60 and 70 cm levels overlap in the 1σ age range, thus the whole sandy interval was deposited rapidly. Considering the ages corresponding to the central point of the 1σ age range, the sedimentation

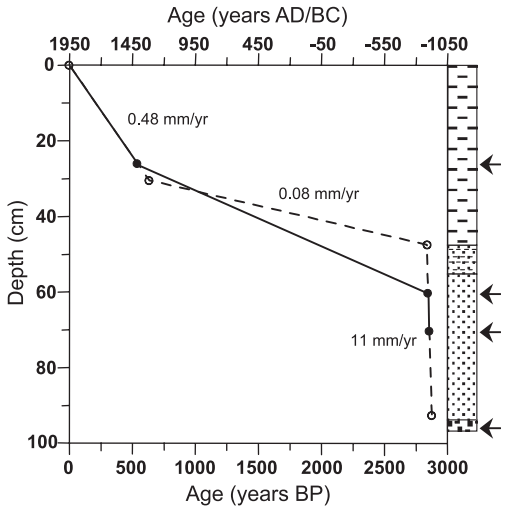

Fig. 3. Age model. Dashed line represents the age model considered in this work. Open circles represent interpolated ages from sedimentation rate estimation. Solid line represents the theoretical age model assuming linear sedimentation rates between ^{14}C dated levels (black circles). Arrows indicate the position of the radiocarbon dated samples. The dated bivalve shell from the core bottom is not included in the age model. ^{14}C ages have been calibrated using Calib 4.3 program (Stuiver et al., 1998a,b). A local reservoir effect of 280±35 radiocarbon years was applied for the uppermost. On the right, a simplified stratigraphic column is shown. Sedimentation rates for each interval, expressed in mm year^{-1}, are indicated on the plot.

rate between 70 and 60 cm is 11 mm year^{-1}. Following the previous discussion, this sedimentation rate has then been applied to the whole glauconitic sand and muddy sand intervals (94–47 cm). According to this logic, the interpolated age at the bottom of the muddy interval is 2835 years BP.

The uppermost dated level is located within the muddy interval. From this level to the core top the sedimentation rate is 0.48 mm year^{-1}. This value was also applied down to 30 cm, where the limit of sedimentary sequences was identified, giving an age for this level of 634 years BP and a sedimentation rate of 0.08 mm year^{-1} for the interval from 47 to 30 cm.

4.4. Carbon, nitrogen and opal distribution

Total carbon distribution is clearly related to sediment grain size. High TC values (2–2.5%) are recorded at the core bottom and through the upper muddy interval, whereas low values (1.5%) are found in the sandy interval (Fig. 4a). The basal maximum can be explained by the accumulation of mollusc fragments and the consequent high content of $CaCO_3$ (17%, Fig. 4b), whereas high values in the upper part are related to organic carbon-rich muddy sediments. In fact, the TOC curve shows low values (0.6%) from the bottom to 60 cm, a sharp increase coinciding with the muddy sand interval and high and relatively constant values (1.6%) in the upper half of the core (Fig. 4c). Therefore, TOC represents half of the TC content in the sandy sediments, although in muddy sediments carbon mostly originates from organic sources. Thus, in the muddy interval, calcium carbonate percentage represents a minor source of TC, showing a relatively stable profile with mean values about 5% (Fig. 4b).

TN follows a similar distribution pattern to TOC. The TN profile can be separated into two intervals, registering values below 0.05% in the sandy interval and higher mean values (0.12%) in the upper half of the core. Increasing values from 60 to 50 cm roughly coincide with the muddy sand interval (Fig. 4d).

TOC and TN values were used to calculate the atomic C/N ratio (Fig. 4e). A relatively stable trend was found throughout the whole core (averaging 13), only interrupted by three peaks of 20.5, 25.4 and 16.8 at 92.5, 75 and 65 cm, respectively.

The final biogeochemical parameter analysed is opal content in the <63-μm fraction (Fig. 4f). Opal

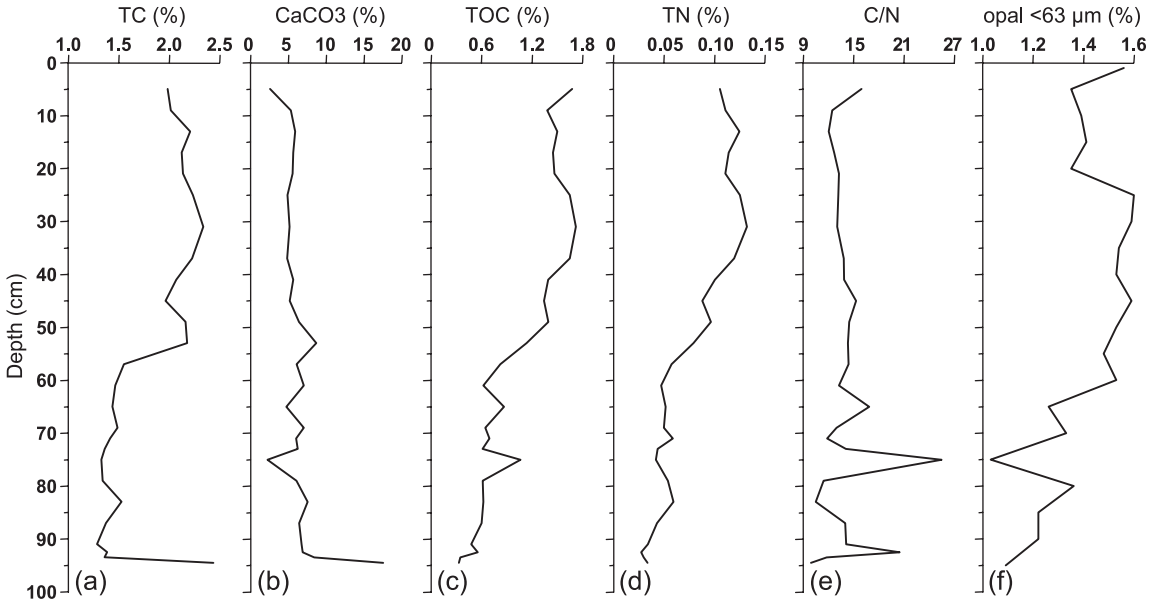

Fig. 4. Profiles of geochemical parameters versus depth. (a) Total carbon content (TC), (b) calcium carbonate content ($CaCO_3$), (c) total organic carbon content (TOC), (d) total nitrogen content (TN), (e) C/N ratio and (f) opal content in fraction <63-μm.

presents an irregular distribution from the bottom to 60 cm, as seen for previous proxies, although an increasing trend may be inferred through this interval. Furthermore, relatively low opal percentages coincide with higher values of C/N ratio. A second interval from 60 to 25 cm characterized by stable values of approximately 1.6% is followed by a decrease down to 1.4% in the uppermost centimetres.

4.5. Planktonic foraminifera

Planktonic foraminifera average 28% of the total foraminiferal fauna. The abundance of planktonic foraminifera per gram of bulk dry sediment averages 600 PF/g in the lower half of the core, rising to a maximum of 1000 PF/g at 80 cm. Abundance decreases in the muddy sand interval, stabilising at about 200 PF/g from 45 cm up to the top of the core. Abundance of benthic foraminifera follows the same pattern, although registering higher values than those of planktonic foraminifera in all samples. Abundances up to 1700 BF/g are reached in the lower half of the core (Fig. 5a). However, if the planktonic foraminiferal abundance is expressed as number of individuals per gram of the >125-μm fraction, a different pattern is observed. In this case, PF/g >125-μm values are relatively low from the bottom to 30 cm, where a sharp increase up to 6300 PF/g was recorded (Fig. 5b). This fact reveals strong planktonic foraminiferal dilution by quartz and glauconite grains in the lower sequence, whereas the medium sand fraction from the upper sequence is mainly constituted by foraminifera.

Twenty three species of planktonic foraminifera are represented in the core. However, four species dominate the assemblages, making up 90% of the total planktonic foraminifera. These taxa include *N. eogloboquadrina pachyderma* (Ehrenberg), *G. lobigerina bulloides* d'Orbigny, *Globigerinita glutinata* (Egger) and *Globorotalia inflata* d'Orbigny.

N. pachyderma (right-coiling) is the most abundant species throughout the whole record. Its mean abundance is 44%, although relatively low percentages are registered at different levels 95, 70, 60 and 45 cm (38%, 39%, 39% and 38%, respectively, Fig. 6a). *G. bulloides* is the second most common species, showing percentages close to the mean value (22%), except for the level located at 25 cm where it reaches

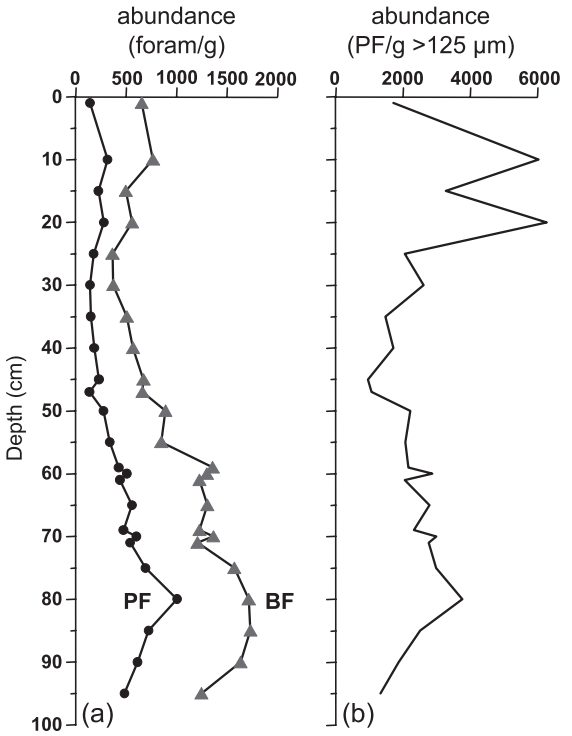

Fig. 5. (a) Abundance of planktonic (PF) and benthic (BF) foraminifera expressed as number of individuals per gram of bulk dry sediment. (b) Abundance of planktonic foraminifera (PF) per gram of >125-μm dry sediment.

maximum abundance (40%) (Fig. 6b). *G. glutinata* is more frequent in the sandy interval (averaging 20%) than in the muddy sediments (averaging 12%), where it registers a minimum value (5%) coinciding with the maximum of *G. bulloides* (Fig. 6c). Mean values of *G. inflata* (9%) are noticeably lower than the previous three species (Fig. 6d).

N. pachyderma (left-coiling), *Globigerina quinqueloba* Natland, *Globigerinoides ruber* (d'Orbigny) and *Globorotalia truncatulinoides* (d'Orbigny) are also registered throughout the whole record, although their mean concentrations range between 1% and 2%. Some other species found in the whole core but never reaching concentrations higher than 1% include: *Globigerinella aequilateralis* (Brady), *Globigerinoides sacculifer* (Brady), *Globigerinella calida* (Parker), *Orbulina universa* d'Orbigny and *Globigerina falconensis* Blow. Sporadically, *Globigerina rubescens* Hofker, *Globorotalia crassaformis* (Galloway and Wissler), *Globorotalia scitula* (Brady),

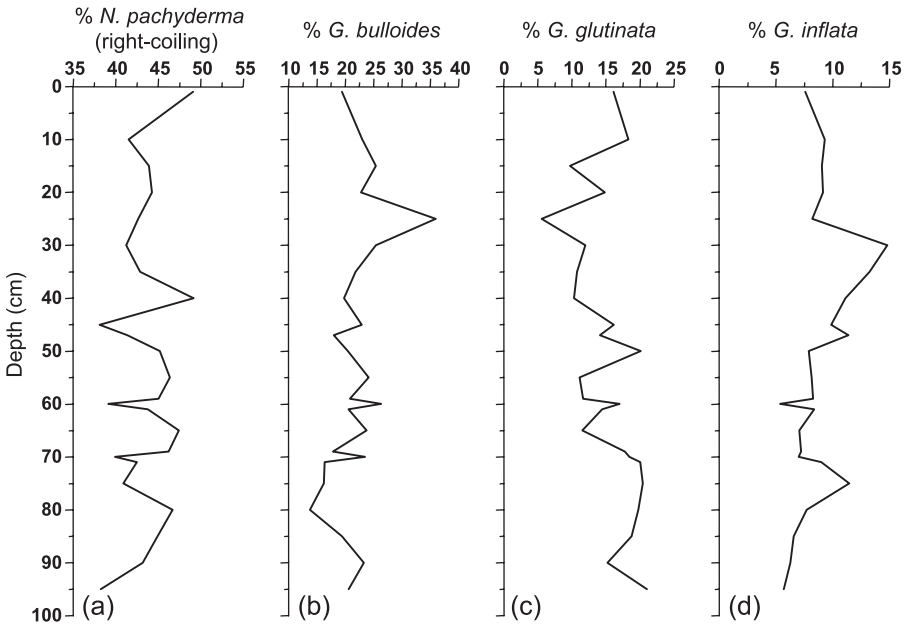

Fig. 6. Percentage versus depth of the most abundant planktonic foraminiferal species. (a) *N. pachyderma* (right-coiling), (b) *G. bulloides*, (c) *G. glutinata* and (d) *G. inflata*.

Globorotalia hirsuta (d'Orbigny), *Globorotalia anfracta* Parker, *Globorotalia ungulata* Bermudez, *Globigerinoides tenellus* Parker, *Turborotalia humilis* (Brady), *Pulleniatina obliquiloculata* (Parker and Jones) and *Globigerinita uvula* (Ehrenberg) are also recorded.

5. Discussion

Sharp lithological contrasts recorded in the core and the trends of most measured variables (TC, TOC, TN, opal and foraminiferal abundance) indicate the existence of two distinct intervals with different environmental conditions in the study region during the last 3000 years. Throughout the sandy interval low TC, TN and opal levels are recorded, whereas in the muddy interval high values of these parameters occur from about 2800 cal. BP to present.

The age model previously discussed indicates that the sand recorded in the lower half of the core may have been deposited rapidly, and in this sense certain intervals can be considered as near-instantaneous deposits. In order to deposit sand layers on a highstand outer continental shelf, high energy processes must be invoked. In particular, we consider these sediments to include a significant component of storm sedimentation. This assumption is supported by the following sedimentological, micropaleontological and biogeochemical features of the deposit.

The basal core comprising sandy bioclastic gravel (Fig. 2) can be explained as a lag deposit partially constituted by reworked shells. Alternatively, there may be a stratigraphic discontinuity between the gravel and overlying sand deposits caused by rapid Holocene Flandrian transgression with the hiatus extending from the end of the Younger Dryas until ca. 2850 cal. BP.

From the core bottom the percentage of sand fraction decreases upwards and a parallel increase of silt and clay sizes are recorded, indicating a progressive decline of energy in the benthic boundary layer. The blurred low-angle lamination observed in this interval suggests that currents were periodically sufficiently strong to develop bedforms but a pervasive bioturbation masks the structures and makes it difficult to determine likely flow characteristics. Some intensely bioturbated intervals show a segregation of grain sizes in X-ray radiographies seen as irregular muddy and sandy pockets. Those

resemble descriptions by Johnson and Baldwin (1996) considered typical for sequences of modern shelf storm deposits.

The mineralogy of the sand fraction clearly reveals that this interval has been reworked. The most frequent grains are rounded quartz, glauconite, foraminifera and echinoderms, bivalves and sponge spicules remains. It is common to find many bioclasts partially filled or completely replaced by glauconite. In other cases, it is easy to identify glauconite as the infilling of foraminiferal chambers, mainly planktonic ones. Glauconite of the Galician continental shelf has previously been studied in detail by Odin and Lamboy (1988). These authors pointed out the inverse relationship between the abundance of carbonate and that of glauconite since the glauconitization process mostly occurs at the expense of carbonate bioclasts. The age of a large proportion of the glauconite obtained by Odin and Lamboy (1988) using K–Ar radiometric dating is between 5 and 6 Ma and thus constitutes relict sediments related either to the late Miocene regressive period or to the general transgression identified on the Iberian Margin at the beginning of Pliocene. The mineralogical composition of this sandy sequence indicates that the sediment is a palimpsest deposit, as pointed out by Bao et al. (1997) who described a mixture of benthic freshwater and marine pelagic diatoms assemblage in the western Galician shelf.

The planktonic foraminiferal assemblages studied in this work constitute a parauthoctonous fauna. The most abundant species from the sand layer, *N. pachyderma* (right-coiling), *G. bulloides* and *G. glutinata*, are the same that those found in the upper muddy interval (Fig. 6). All of them are typical species from subpolar and transitional assemblages inhabiting this region (Bé, 1977; Levy et al., 1995; Cayre et al., 1999). Planktonic foraminiferal abundance is two or even three times lower than the benthic one in the sandy interval (Fig. 5a). The ratio of planktonic foraminifera/benthic foraminifera (PF/BF) has previously been used as a paleobathymetry proxy (Boersma, 1998), and although the ratio can not be considered to have a linear relationship with bathymetry, higher abundance of benthic foraminifera suggests that individuals have been transported from the inner shelf. This hypothesis is supported by the preservation of foraminiferal tests: whilst planktonic individuals are moderate to well preserved, many benthic microfossils are fragmented.

The reworked origin of the sand layer is also supported by the C/N ratio (Fig. 4e). Although C/N measurements are not unequivocal in distinguishing degraded marine plankton from terrestrial material (Tyson, 1995; Johnson and Grimm, 2001), this ratio has been frequently employed as an indirect marker of organic matter provenance (Meyers, 1992; den Dulk et al., 1998; Cowie et al., 1999; Meyers and Doose, 1999; Bhushan et al., 2001). Meyers and Doose (1999) suggested that algae typically have atomic C/N values between 4 and 10, whereas vascular land plants have C/N values of 20 and greater (Emerson and Hedges, 1988; Meyers, 1994). In general, throughout the whole core, C/N ratio falls into the range of 10–16, indicating that organic matter is predominantly of marine origin (Calvert et al., 1995) or a mixture of carbon from various terrestrial and marine sources (Leithold and Hope, 1999). However, three prominent C/N peaks at 92, 75 and 65 cm coincide with low opal contents (Fig. 4f). These peaks suggest stronger terrestrial contribution. The chief mechanism able to bring terrestrial organic carbon to the outer shelf are turbid plumes issuing from extreme river discharges (wind-driven currents and offshore winds are not strong enough to be invoked due to the hydrographic and climatic settings).

According to the above discussion, we interpret our data to indicate that the predominantly sandy facies in the lower half of the core were deposited by periodic storm currents (Aigner and Reineck, 1982) between fair-weather wave base and storm wave base at ca. 2850 cal. BP. Under these conditions, high-amplitude surface waves stirred the inner shelf sea floor and resuspended previously deposited sediments which were then carried to the outer shelf by low density flows (Harms et al., 1982), allowing for the mixing of continental and marine material. This is consistent with other recorded storm deposits identified in the Ría de Pontevedra, close to the core position (García-Gil et al., 1999).

The sandy interval is overlain with a profusely bioturbated muddy sand interval 10 cm thick. All analysed markers show a pronounced shift throughout this interval. Mixing of sand and mud is thought to have been largely accomplished by the post-storm activities of benthic organisms (Harms et al., 1982).

The upper muddy interval strongly contrasts with the underlying levels. The samples from the muddy and sandy intervals can be easily distinguished also by their TOC percentage and, to a lesser extent, by their $CaCO_3$ content (Fig. 7). The muddy interval is characterised by higher TOC and slightly lower $CaCO_3$ contents. This correlation of organic carbon accumulation and preservation with fine grain size deposition indicates a substantially lower energy level (Fig. 7b).

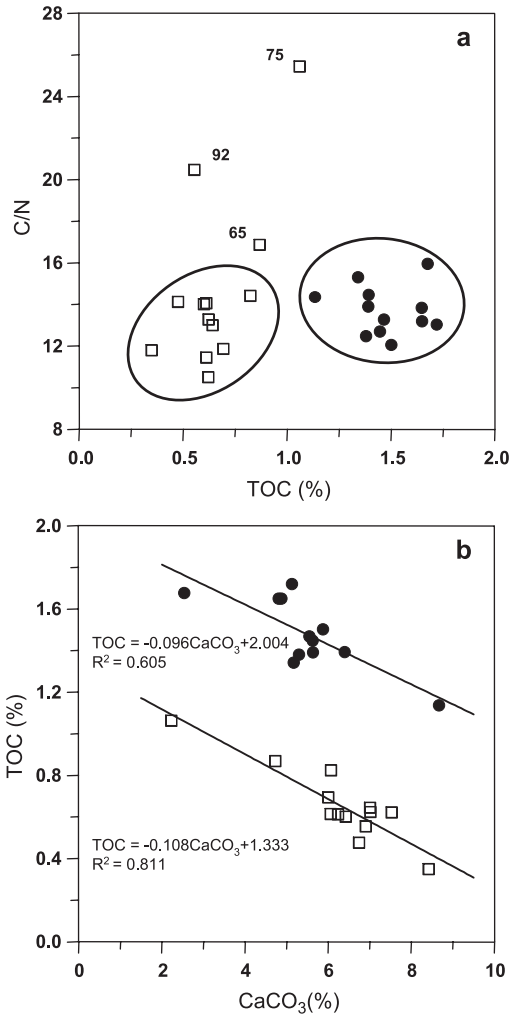

Fig. 7. (a) Plot of C/N ratio as a function of TOC. Numbers beside the squares indicate the position in the core (in cm). (b) Variations of TOC with $CaCO_3$. Solid lines represent the linear regression between parameters. Open squares represent samples from sandy interval. Solid circles represent samples from muddy interval. Equations and R^2 are also indicated.

The sharp sedimentary change observed at 47 cm represents the transition from a storm-dominated shelf to a shelf characterised by low-energy environmental conditions. We have estimated that the change took place between 885 and 756 cal. BC, coincident with the age proposed by van Geel et al. (1996) for the Subboreal/Subatlantic transition (850–760 cal. BC). This transition is characterised by a sharp rise of atmospheric $\Delta^{14}C$ content, caused by a sudden decline of solar activity (Kilian et al., 1995; van Geel et al., 1999) leading to a strong shift from relatively continental (warm and dry) to a more oceanic climate regime (cool and wetter). The climate instability associated with the Subboreal/Subatlantic transition was linked to an intensification of mid-latitude storm tracks (van Geel et al., 2001). It is possible that the sand layer interpreted as a series of storm deposits may have accumulated during this period, although the para-utochthonous planktonic microfauna is as much as 140 years older than the age of the Subboreal/Subatlantic transition.

The upper muddy interval shows a homogeneous character. Its grain size and micropaleontological features indicate that it was deposited mainly by settling processes. Consequently, the analysed markers can be used as paleoproductivity and surface water dynamics proxies. Throughout the muddy interval, most records clearly show a constant trend, suggesting a relatively stable environment. TOC, TN and opal record high values, reaching the highest percentage along with the maximum clay content (Fig. 4c, d and f). Opal content in sediments is an important paleoproductivity proxy (Ragueneau et al., 2000), especially in the study region where biogenic opal is dominated by diatoms (Bode et al., 1994; Bao et al., 1997; Tilstone et al., 2000). Johnson and Grimm (2001) found a positive linear association between TOC and opal content in marine sediments, because the growth of diatoms involves the production of both opal and organic carbon. A link between TOC and opal content is found in the upper part of the studied core indicating that productivity is enhanced at these levels. The C/N ratio shows a very stable pattern with relatively low values suggesting that productivity was predominantly of marine origin (Fig. 4e).

We conclude that the whole muddy interval was deposited in a relatively stable marine environment where terrestrial and shallow marine influences were

negligible. These environmental conditions are similar to those found on the present outer shelf. Planktonic foraminiferal assemblages close to those inhabiting this region today also support this interpretation. Planktonic foraminiferal species show a latitudinal distribution pattern mainly reflecting the influence of subsurface water temperature. As a consequence, various microfaunal provinces can be distinguished, i.e., arctic–antarctic, subarctic, transitional, subtropical and tropical (Bé, 1977). Close to the studied area, in the Iberian Margin off Portugal, Cayre et al. (1999) described three assemblages: subtropical, transitional and subpolar. In this work, we have employed the assemblages defined by Cayre et al. (1999) distinguishing also a subpolar *s.s.* assemblage composed by *N. pachyderma* (left-coiling) and *G. quiqueloba* (Fig. 8).

Despite the general stability described for the muddy interval, the opal content, the foraminiferal abundance and their assemblages allow identification of different hydrographic patterns during the last 2800 years. From 885 cal. BC to 1420 AD, the opal content records constant high values, but foraminifera are relatively scarce. From 1420 AD to present, the opal content is also constant but a 20% lower than the previous period and foraminifera are abundant, mainly if we consider the >125-μm fraction (Figs. 4f and 5b).

The planktonic foraminiferal assemblage which dominates the rich-opal interval is the transitional one (Fig. 8c). Species included in this assemblage are related to the subtropical gyre margin and are most frequent nowadays in this mid-latitude region. The assemblage records a pronounced decrease at 1420 AD, when the subpolar assemblage (Fig. 8b) reaches the highest percentage and the opal content starts to decrease. The increase of subpolar species, solely due to a sharp increase in *G. bulloides* (Fig. 6b), replacing partially the transitional assemblage, and the lowest percentage of the subtropical assemblage reveal the incursion of colder waters. *G. bulloides* is also regarded as typical species from upwelling areas (Thiede and Jünger, 1992). Therefore, the abundance of planktonic foraminifera (Fig. 5b) and the composition of their assemblages (Fig. 8) are responding to a short but intense upwelling of colder intermediate waters. Soares (1993) in the Portuguese margin and Diz et al. (2002) in the Galician Rías Baixas recognized an intensification of the upwelling regime at the beginning of the last millennium. In the studied core, the age of the upwelling event falls within the

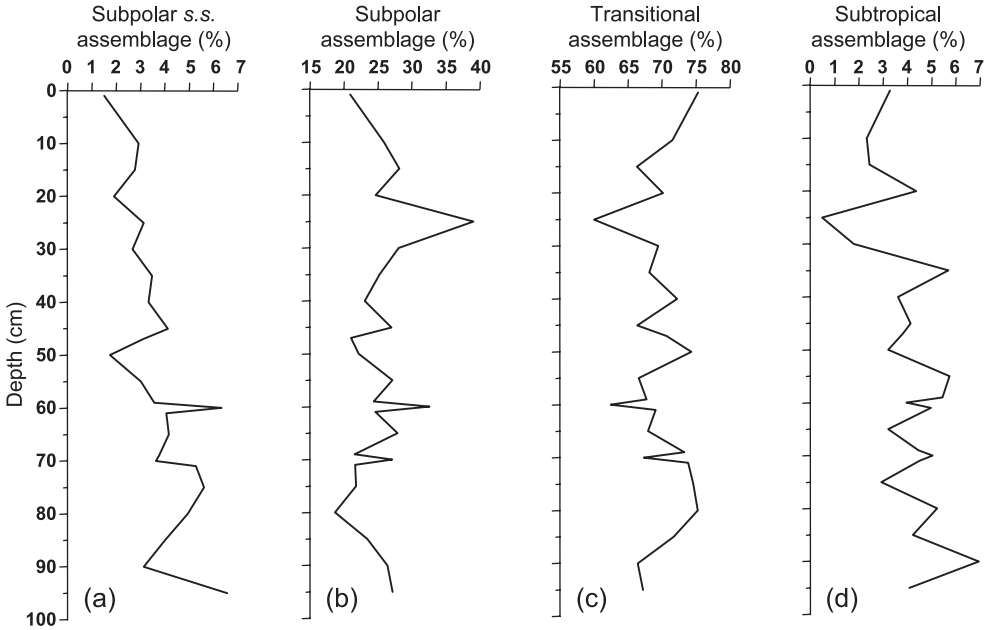

Fig. 8. Percentages versus depth of the four assemblages defined in this work. (a) Subpolar *s.s.* assemblage, (b) subpolar assemblage, (c) transitional assemblage and (d) subtropical assemblage.

age range of the LIA, in agreement with the conclusion obtained by Diz et al. (2002). According to these authors, a decrease of 2 °C in sea surface temperature evidenced in the Ría de Vigo at the same time reflects the combined effect of emerging cold waters from the upwelling and colder atmospheric temperatures.

According to Soares (1993) and Diz et al. (2002), the upwelling regime has prevailed in this region until present. In fact, the most conspicuous characteristic of the present hydrography of the region is the existence of a seasonal upwelling during summer (Fraga, 1981). In the studied core lower opal percentages are recorded during the last centuries. The presence of upwelling does not indicate that enhanced storage of biogenic silica be occurring in bottom sediments. This apparent contradiction may be understood by considering an increase in shelf current upwelling. This would also enhance the transport offshore in both phytoplankton and organic matter (Estrada, 1984; Varela, 1990; López-Jamar et al., 1992) away from the core site. Another important process is the remineralization taking place in the region during present upwelling pulses. Maximum remineralization occurs at 90–130 m depth along with maximum nutrient and oxygen depletion (Prego et al., 1999). Thus, the biogenic silica remineralization could actually be enhanced in the core area (Prego and Bao, 1997).

6. Conclusions

During the last 3000 years, two periods with contrasted environmental conditions have been identified in the western Galician continental shelf. The most pronounced environmental change took place at 2850 cal. BP, coinciding with the Subboreal/Subatlantic transition. This transition represents a climate instability period that was accompanied by high storminess in mid-latitudes. Sedimentation on the western Galician shelf is interpreted to have been controlled by this storm regime. Strong offshore bottom currents caused by storms are considered to have been responsible for deposition of a palimpsest deposit 50 cm thick on the outer shelf.

The onset of the Subatlantic involved the establishment of low energy conditions on the outer continental shelf, where predominately fine sediments were deposited. This period shows a relative environmental stability, but the regional hydrography may have experienced a change at 1420 AD when an incursion of colder water planktonic foraminifera reveals an upwelling pulse, probably reinforced by colder atmospheric temperatures during the LIA. Once the cold conditions related to the LIA had ended, temperate planktonic foraminifera became dominant again. The seasonal upwelling regime has prevailed until present days affecting to the continental shelf. Regardless of enhanced productivity, lesser amount of opal is preserved in recent outer shelf sediments due to offshore transport and stronger remineralization.

Acknowledgements

We thank S. Rúa-Santerbás and M. Martínez-García their help with sample processing and the Mytilus crew for help in core collection. A.W. Dale and K. Rea were of great help in making language corrections. We are indebted to M. Pérez-Arlucea for her helpful critical comments on this paper. Very constructive reviews by F.J. Sierro and M. Leeder are sincerely acknowledged. R.G.A. and P.B. acknowledge Ministerio de Educación, Cultura y Deportes and Xunta de Galicia for doctoral grants. This work was funded by REN2000-1102 MAR, PGIDT00-MAR30103PR and PGIDT00PXI30105PR Projects. Contribution to IGCP-464, 244 of the EX1 group of the University of Vigo.

References

Aigner, T., Reineck, H.-E., 1982. Proximality trends in modern storm sands from the Helgoland Bight (North Sea) and their implications for basin analysis. Senckenbergiana Maritima, 14, 183–215.

Bao, R., Varela, M., Prego, R., 1997. Mesoscale distribution patterns of diatoms in surface sediments as tracers of coastal upwelling of the Galician shelf (NW Iberian Peninsula). Marine Geology, 144, 117–130.

Barber, K.E., Maddy, D., Rose, N., Stevenson, A.C., Stoneman, R., Thompson, R., 2000. Replicated proxy-climate signals over the last 2000 yr from two distant peat bogs: new evidence for regional palaeoclimate teleconnections. Quaternary Science Reviews, 19, 481–487.

Bé, A.W.H., 1977. An ecological, zoogeographic and taxonomic review of recent planktonic foraminifera. Ramsay, A.T.S. (Ed.), Oceanic Micropaleontology, vol. 1. Academic Press, London, pp. 1–100.

Bhushan, R., Dutta, K., Somayajulu, B.L.K., 2001. Concentrations and burial fluxes of organic and inorganic carbon on the eastern margins of the Arabian Sea. Marine Geology, 178, 95–113.

Bianchi, G.G., McCave, I.N., 1999. Holocene periodicity in North Atlantic climate and deep-ocean flow south of Iceland. Nature, 397, 515–517.

Blanton, J.O., Atkinson, L.P., Fernández de Castillejo, F., Lavin, A., 1984. Coastal upwelling of the Rías Bajas, Galicia, northwest Spain: I. Hydrographic studies. Rapports et Proces Vervaux des Reunions-CIESM, 183, 79–90.

Bode, A., Casas, B., Varela, M., 1994. Size-fractionated primary productivity and biomass in the Galician shelf (NW Spain): net plankton versus nanoplankton dominance. Scientia Marina, 58, 131–141.

Boersma, A., 1998. Foraminifera. In: Haq, B.U., Boersma, A. (Eds.), Introduction to Marine Micropaleontology. Elsevier, Singapore, pp. 19–77.

Bond, G., Showers, W., Cheseby, M., Lotti, R., Almasi, P., deMenocal, P., Priore, P., Cullen, H., Hajdas, I., Bonani, G., 1997. A pervasive millenial-scale cycle in North Atlantic Holocene and glacial climates. Science, 278, 1257–1266.

Calvert, S.E., Pedersen, T.F., Naidu, P.D., von Stackelberg, U., 1995. On the organic carbon maximum on the continental slope of the eastern Arabian Sea. Journal of Marine Research, 53, 269–296.

Campbell, I.D., Campbell, C., Apps, M.J., Rutter, N.W., Bush, A.B.G., 1998. Late Holocene ~1500 yr climatic periodicities and their implications. Geology, 26, 471–473.

Cayre, O., Lancelot, Y., Vicent, E., Hall, M.A., 1999. Paleoceanographic reconstructions from planktonic foraminifera off the Iberian Margin: temperature, salinity and Heinrich events. Paleoceanography, 14, 384–396.

Cowie, G.L., Calvert, S.E., Pedersen, T.F., Schulz, H., von Rad, U., 1999. Organic content and preservational controls in surficial shelf and slope sediments from the Arabian Sea (Pakistan margin). Marine Geology, 161, 23–38.

Dahl-Jensen, D., Mosegaard, K., Gundestrup, N., Clow, G.D., Johnsen, S.J., Hansen, A.W., Balling, N., 1998. Past temperatures directly from Greenland ice sheet. Science, 282, 268–271.

deMenocal, P., Ortiz, J., Guilderson, T., Sarnthein, M., 2000. Coherent high-and low-latitude climate variability during the Holocene warm period. Science, 288, 2198–2202.

den Dulk, M., Reichart, G.J., Memon, G.M., Roelofs, E.M.P., Zachariasse, W.J., van der Zwaan, G.J., 1998. Benthic foraminifera response to variations in surface water productivity and oxygenation in the northern Arabian Sea. Marine Micropaleontology, 35, 43–66.

Diz, P., Francés, G., Pelejero, C., Grimalt, J.O., Vilas, F., 2002. The last 3000 years in the Ría de Vigo (NW Iberian Margin): climatic and hydrographic signals. Holocene, 12, 459–468.

Edwards, T.W.D., Graf, W., Trimborn, P., Stichler, W., Lipp, J., Payer, H.D., 2000. $\delta^{13}C$ response surface resolves humidity and temperature signals in trees. Geochimica et Cosmochimica Acta, 64, 161–167.

Emerson, S., Hedges, J.I., 1988. Processes controlling the organic carbon content of open oceans sediments. Paleoceanography, 3, 621–634.

Estrada, M., 1984. Phytoplankton distribution and composition off the coast of Galicia (Northwest of Spain). Journal of Plankton Research, 6, 417–434.

Fiúza, A.F.G., 1984. Hidrologia e dinâmica das águas costeiras de Portugal. PhD thesis. Universidade de Lisboa, Portugal, unpublished (in Portuguese).

Fraga, F., 1981. Upwelling off the Galician coast, Northwest of Spain. In: Richards, F.A. (Ed.), Coastal Upwelling. American Geophysical Union, Washington, DC, pp. 176–182.

Frouin, R., Fiúza, A.F.G., Ambar, I., Boyd, T.J., 1990. Observations of a poleward surface current off the coasts of Portugal and Spain during winter. Journal of Geophysical Research, 95, 679–691.

García-Gil, S., Vilas, F., García-García, A., Durán, R., 1999. Holocene storm delta in incised-valley fill sediments of Ria de Pontevedra, NW Spain. EOS Transactions, 80, F559.

Hansen, H.P., Grashoff, K., 1983. Automated chemical analysis. In: Grashoff, M., Ehrhardt, M., Kremlin, K. (Eds.), Methods of Seawater Analysis. Verlag Chemie, Weinheim, pp. 368–376.

Harms, J.C., Southard, J.B., Walker, R.G., 1982. Structures and Sequences in Clastic Rocks, SEPM Short Course, vol. 9. Society of Economic Paleontologists and Mineralogists, Tulsa, OK.

Haynes, R., Barton, E.D., Pilling, I., 1993. Development, persistence, and variability of upwelling filaments off the Atlantic Coast of the Iberian Peninsula. Journal of Geophysical Research, 98, 22681–22692.

Johnson, H.D., Baldwin, C.T., 1996. Shallow clastic seas. In: Reading, H.G. (Ed.), Sedimentary Environments: Processes, Facies and Stratigraphy. Blackwell Science, Oxford, pp. 232–280.

Johnson, K.M., Grimm, K.A., 2001. Opal and organic carbon in laminated diatomaceous sediments: Saanich Inlet, Santa Barbara Basin and Miocene Monterey Formation. Marine Geology, 174, 159–175.

Keigwin, L.D., 1996. The Little Ice Age and the Medieval Warm Period in the Sargasso Sea. Science, 274, 1504–1508.

Kennett, J.P., Srinivasan, M.S., 1983. Neogene Planktonic Foraminifera. A Phylogenetic Atlas. Hutchinson Ross, Stroudsburg, Pennsylvania.

Kilian, M.R., van der Plitch, J., van Geel, B., 1995. Dating raised bogs: new aspects of AMS ^{14}C wiggle matching, a reservoir effect and climate change. Quaternary Science Reviews, 14, 959–966.

Kreutz, K.J., Mayewski, P.A., Meeker, L.D., Twickler, M.S., Whitlow, S.I., Pittalwala, I.I., 1997. Bipolar changes in atmospheric circulation during the Little Ice Age. Science, 277, 1294–1296.

Lamb, H.H., 1995. Climate History and the Modern World. Routledge, London.

Leithold, E.L., Hope, R.S., 1999. Deposition and modification of a flood layer on the northern California shelf: lessons from and

about the fate of terrestrial particulate organic carbon. Marine Geology, 154, 183–195.

Levy, A., Mathieu, R., Poignant, A., Rosset-Moulinier, M., Ubaldo, M.L., Lebreiro, S., 1995. Foraminifers Actuels de la Marge Continentale Portugaise—Inventaire et Distribution. Memórias do Instituto Geológico e Mineiro, Lisbon, 116 pp. (in French).

López-Jamar, E., Cal, R.M., González, G., Hanson, R.B., Rey, J., Santiago, G., Tenore, K.R., 1992. Upwelling and outwelling effects on the benthic regime of the continental shelf off Galicia, NW Spain. Journal of Marine Research, 50, 465–488.

McManus, J., 1991. Grain size determination and interpretation. In: Tucker, M. (Ed.), Techniques in Sedimentology. Blackwell Scientific Publications, Oxford, pp. 63–85.

Meese, D.A., Gow, A.J., Grootes, P., Mayewski, P.A., Ram, M., Stuiver, M., Taylor, K.C., Waddington, E.D., Zielinski, G.A., 1994. The accumulation record from the GISP2 core as an indicator of climate change throughout the Holocene. Science, 266, 1680–1682.

Meyers, P.A., 1992. Organic matter variations in sediments from DSDP sites 362 and 532: evidence of changes in the Benguela Current upwelling system. In: Summerhayes, C.P., Prell, W.L., Emeis, K.C. (Eds.), Upwelling Systems: Evolution Since the Early Miocene. Special Publication-Geological Society of London, vol. 64, pp. 323–329.

Meyers, P.A., 1994. Preservation of elemental and isotopic source identification of sedimentary organic matter. Chemical Geology, 114, 289–302.

Meyers, P.A., Doose, H., 1999. Sources, preservation, and thermal maturity of organic matter in Pliocene–Pleistocene organic-carbon-rich sediments of the western Mediterranean sea. In: Zahn, R., Comas, M.C., Klaus, A., (Eds.), Proceedings of the Ocean Drilling Program, Scientific Results, vol. 161. Ocean Drilling Program, College Station, TX, pp. 383–390.

Mortlock, R., Fröelich, P.N., 1989. A simple method for the rapid determination of biogenic opal in pelagic marine sediments. Deep-Sea Research, 36, 1415–1426.

O'Brien, S.R., Mayewski, P.A., Meeker, L.D., Meese, D.A., Twickler, M.S., Whitlow, S.I., 1995. Complexity of Holocene climate as reconstructed from a Greenland ice core. Science, 270, 1962–1964.

Odin, G.S., Lamboy, M., 1988. Glaucony from the margin off northwestern Spain. In: Odin, G.S. (Ed.), Green Marine Clays: Oolitic Ironstone Facies, Verdine Facies, Glaucony Facies and Celadonite-bearing Facies—A Comparative Study. Elsevier, Amsterdam, pp. 249–275.

Prego, R., Bao, R., 1997. Upwelling influence on the Galician coast: silicate in shelf water and underlying surface sediments. Continental Shelf Research, 17, 307–318.

Prego, R., Varela, M., 1998. Hidrography of the Artabro Gulf in summer: western coastal limit of Cantabrian seawater and wind-induced upwelling at Prior Cape. Oceanologica Acta, 21, 145–155.

Prego, R., Barciela, C., Varela, M., 1999. Nutrient dynamics in the Galician coastal area (Nortwestern Iberian Peninsula): do the Rias Bajas receive more nutrient salts than the Rias Altas? Continental Shelf Research, 19, 317–334.

Ragueneau, O., Tréguer, P., Leynaert, A., Anderson, R.F., Brzezinski, M.A., DeMaster, D.J., Dugdale, R.C., Dymond, J., Fischer, G., François, R., Heinze, C., Maier-Reimer, E., Martin-Jézéquel, V., Nelson, D.M., Quéguiner, B., 2000. A review of the Si cycle in the modern ocean: recent progress and missing gaps in the application of biogenic opal as a paleoproductivity proxy. Global and Planetary Change, 26, 317–365.

Reimer, P., 2001. Marine Reservoir Correction Database. WWW Page, http://depts.washington.edu/qil/marine.

Rey, J., 1993. Relación Morfosedimentaria entre la Plataforma Continental de Galicia y las Rías Bajas y su Evolución durante el Cuaternario. Publicaciones Especiales-Instituto Español de Oceanografía, 17, 233 pp. (in Spanish).

Ríos, A.F., Pérez, F.F., Fraga, F., 1992. Water masses in the upper and middle North Atlantic Ocean east of the Azores. Deep-Sea Research, 39, 645–658.

Rolán-Mosquera, E., Otero-Schmitt, J., Rolán-Álvarez, E., 1989. Moluscos de la Ría de Vigo II. Thalassas. Revista de Ciencias del Mar, Anexo, vol. 2. Servicio de Publicacións e Intercambio Científico da Universidade de Santiago de Compostela, Santiago de Compostela (in Spanish).

Soares, A.M., 1993. The ^{14}C content on marine shells: evidences for variability in coastal upwelling off Portugal during the Holocene. Proceedings of an International Symposium on Applications of Isotope Techniques in the Studying Past and Current Environmental Changes in the Hydrosphere and the Atmosphere. International Atomic Energy Agency, Vienna, pp. 471–485.

Stuiver, M., Grootes, P.M., Braziunas, T.F., 1995. The GISP2 $\delta^{18}O$ climate record of the past 16,500 years and the role of the sun, ocean, and volcanoes. Quaternary Research, 44, 341–354.

Stuiver, M., Reimer, P.J., Braziunas, T.F., 1998a. High-precision radiocarbon age calibration for terrestrial and marine samples. Radiocarbon, 40, 1127–1151.

Stuiver, M., Reimer, P.J., Bard, E., Beck, J.W., Burr, G.S., Hughen, K.A., Kromer, B., McCormac, F.G., van der Plicht, J., Spurk, M., 1998b. INTCAL98 radiocarbon age calibration 24000–0 BP. Radiocarbon, 40, 1041–1083.

Thiede, J., Jünger, B., 1992. Faunal and flora indicators of coastal upwelling (NW African and Peruvian Continental Margins). Summerhayes, C.P., Prell, W.L., Emeis, K.C. (Eds.), Upwelling Systems: Evolution Since the Early Miocene, vol. 64. Geological Society Special Publications, London, pp. 47–76.

Tilstone, G.H., Míguez, B.M., Figueiras, F.G., Fermín, E.G., 2000. Diatom dynamics in a coastal ecosystem affected by upwelling: coupling between species succession circulation and biogeochemical processes. Marine Ecology Progress Series, 205, 23–41.

Tyson, R.V., 1995. Sedimentary Organic Matter. Chapman and Hall, London.

van Geel, B., Buurman, J., Waterbolk, H.T., 1996. Archaeological and palaeoecological indications of an abrupt climate change in The Netherlands, and evidence for climatological teleconnections around 2650 BP. Journal of Quaternary Science, 11, 451–460.

van Geel, B., Raspopov, O.M., Renssen, H., van der Plicht, J., Dergachev, V.A., Meijer, H.A.J., 1999. The role of solar

forcing upon climate change. Quaternary Science Reviews, 18, 331–338.

van Geel, B., Renssen, H., van der Plicht, J., 2001. Evidence from the past: solar forcing of climate change by way of cosmic rays and/or by solar UV? In: Kirkby, J. (Ed.), Proceedings of the Workshop on Ion–Aerosol–Cloud Interactions. CERN, Geneva.

Varela, M., 1990. Upwelling and phytoplankton ecology in Galician (NW Spain) Rías and shelf waters. Boletín del Instituto Español de Oceanografía, 8, 57–74.

Wooster, W.S., Bakun, A., McClain, D.R., 1976. The seasonal upwelling cycle along the eastern boundary of the North Atlantic. Journal of Marine Research, 34, 131–141.